The Journal of Neuroscience, October 15, 2002, 22(20):8808–8818

Neuronal Premotor Networks Involved in Eyelid Responses: Retrograde Transneuronal Tracing with Rabies Virus from the Orbicularis Oculi Muscle in the Rat

Sara Morcuende,[1] José-Maria Delgado-García,[1] and Gabriella Ugolini[2]

[1]*Laboratorio Andaluz de Biología, Universidad Pablo de Olavide, 41013 Sevilla, Spain, and* [2]*Laboratoire de Virologie Moléculaire et Structurale, Centre National de la Recherche Scientifique, 91198 Gif-sur-Yvette, France*

Retrograde transneuronal tracing with rabies virus from the right orbicularis oculi muscle was used to identify neural networks underlying spontaneous, reflex, and learned blinks. The kinetics of viral transfer was studied at sequential 12 hr intervals between 3 and 5 d after inoculation. Rabies virus immunolabeling was combined with the immunohistochemical detection of choline acetyltransferase expression in brainstem motoneurons or Fluoro-Ruby injections in the rubrospinal tract. Virus uptake involved exclusively orbicularis oculi motoneurons in the dorsolateral division of the facial nucleus. At 3–3.5 d, transneuronal transfer involved premotor interneurons of trigeminal, auditory, and vestibular reflex pathways (in medullary and pontine reticular formation, trigeminal nuclei, periolivary and ventral cochlear nuclei, and medial vestibular nuclei), motor pathways (dorsolateral quadrant of contralateral red nucleus and parарubral area), deep cerebellar nuclei (lateral portion of interpositus nucleus and dorsolateral hump ipsilaterally), limbic relays (parabrachial and Kölliker–Fuse nuclei), and oculomotor structures involved in eye–eyelid coordination (oculomotor nucleus, supraoculomotor area, and interstitial nucleus of Cajal). At 4 d, higher order neurons were revealed in trigeminal, auditory, vestibular, and deep cerebellar nuclei (medial, interpositus, and lateral), oculomotor and visual-related structures (Darkschewitsch, nucleus of the posterior commissure, deep layers of superior colliculus, and pretectal area), lateral hypothalamus, and cerebral cortex (particularly in parietal areas). At 4.5 and 5 d the labeling of higher order neurons occurred in hypothalamus, cerebral cortex, and blink-related areas of cerebellar cortex. These results provide a comprehensive picture of the premotor networks mediating reflex, voluntary, and limbic-related eyelid responses and highlight potential sites of motor learning in eyelid classical conditioning.

Key words: cerebellum; eyelid responses; parietal cortex; rabies virus; rats; red nucleus; reflex blinks; reticular formation

The kinematics and frequency domain properties of eyelid responses have been reported in a quantitative manner for spontaneous, reflex, passive, and learned movements in rabbits, cats, and humans (McCormick et al., 1982; Gormezano et al., 1983; Woody, 1986; Evinger et al., 1991; Welsh, 1992; Thompson and Krupa, 1994; Domingo et al., 1997; Gruart et al., 2000a). The activity of selected neural structures has been related convincingly to different aspects of reflex and learned eyelid responses. Thus, the properties of orbicularis oculi motoneurons involved in eyelid closing have been described previously (Trigo et al., 1999), and a relationship between neural firing responses and eyelid movements has been reported for several brain sites, e.g., red nucleus, cerebellar cortex and nuclei, motor cortex, and hippocampus (Berger et al., 1983; McCormick and Thompson, 1984; Berthier and Moore, 1986, 1990; Aou et al., 1992; Keifer, 1993; Gruart et al., 2000b; Múnera et al., 2001). A map of the sites involved in the generation of classically conditioned eyelid responses has been proposed (Kim and Thompson, 1997) on the basis of lesion or inactivation of given neural structures.

Nevertheless, despite some really valuable attempts (Courville, 1966; Takeuchi et al., 1979; Hinrichsen and Watson, 1983; Travers and Norgren, 1983; Fanardjian and Manvelyan, 1984, 1987a,b; Takada et al., 1984; Holstege et al., 1986a,b; Isokawa-Akesson and Komisaruk, 1987; Fort et al., 1989), available information regarding the organization of the eyelid premotor system is limited. Eyelid movements are specialized motor responses, related not only to corneal protection but also to emotional expression, visual perception, and eye movements and are susceptible to motor learning. Given the diversity of sensory sources able to activate eyelid muscles and the variety of behavioral displays in which they are involved, the underlying neuronal network should be rather complex. A comprehensive map of such networks could not be obtained with conventional tracers (Mesulam, 1982; Kuypers and Huisman, 1984; Köbbert et al., 2000) but now can be accomplished with retrograde transneuronal tracers that are able to reveal neuronal networks in their entirety. The most effective transneuronal tracers are viruses because of their ability to function as self-amplifying markers (Ugolini et al., 1989; Kuypers and Ugolini, 1990; Ugolini, 1995a,b). Rabies virus is the most valuable, particularly for studying motor networks, because after its injection into muscles or nerves it is taken up exclusively by motoneurons, without uptake by sensory or sympathetic neurons (Ugolini, 1995b; Tang et al., 1999; Kelly and Strick, 2000; Graf et al., 2002). Rabies virus propagates exclusively by retrograde transneuronal transfer. Transfer is time-dependent, enabling a sequential visualization of

Received Feb. 26, 2002; revised July 8, 2002; accepted July 22, 2002.

This work was supported by European Union Grant BIO4-CT98-0546. We are grateful to Dr. A. Gruart for her comments and suggestions and to R. Churchill for help in the editing of this manuscript. S.M. was a visiting doctoral fellow at G.U.'s laboratory (fellowship supported by the Spanish Ministerio de Educación y Ciencia program FP-96).

Correspondence should be addressed to Dr. Gabriella Ugolini, Laboratoire de Virologie Moléculaire et Structurale, Institut de Neurobiologie Alfred Fessard, Bâtiment 32, Centre National de la Recherche Scientifique, 91198 Gif-sur-Yvette, France. E-mail: gabriella.ugolini@gv.cnrs-gif.fr.

Copyright © 2002 Society for Neuroscience 0270-6474/02/228808-11$15.00/0

serially connected neurons across an unlimited number of synapses. Rabies-infected neurons remain viable and intact (Ugolini, 1995b; Tang et al., 1999; Graf et al., 2002).

We have exploited this powerful method to study the neural networks controlling the orbicularis oculi muscle. Our results provide a comprehensive map of such networks, showing the involvement of different sensory modalities (trigeminal, vestibular, auditory, and visual) in the genesis and control of eyelid responses and the participation of specific portions of sensorimotor cortex, red nucleus, reticular formation, and cortical and nuclear cerebellar areas.

Some results already have been published in abstract form (Ugolini et al., 1999).

MATERIALS AND METHODS

Viral tracer. The virus used in this study was the challenge virus standard (CVS), fixed strain 11 of rabies virus (Ugolini, 1995b). Concentrated virus [titer 1–1.5 $\times 10^{10}$ plaque-forming units (pfu)/ml] was prepared by pelleting the supernatant of baby hamster kidney-21 (BHK-21) cells infected for 72 hr through a cushion of 25% glycerol. The virus stock was kept frozen at −70°C until a few minutes before use.

Animals, virus injection, and perfusion procedures. Experiments were performed in 55 albino Wistar rats (Iffa Credo, Les Oncins, France), weighing 250–300 gm. Animal care and experimental procedures conformed with French Government, European Union Directive (86/609/EU), and National Institutes of Health guidelines. Surgery was performed aseptically under general anesthesia (Avertin 1.3–1.5 ml/100 gm, i.p., plus supplementary doses as required to maintain areflexia). The right orbicularis oculi muscle was exposed after a sagittal incision of the scalp. Using a glass micropipette connected to a pressure pump, we placed two injections of rabies virus (3–4.5 μl each) into the preseptal and pretarsal portions of the muscle, respectively, to map premotor innervation of both muscle components. The pipette was inserted in the muscle under microscopic guidance and kept in place for 5 min after each injection. Any eventual leakage of the inoculum was removed with cotton swabs. The wounds were sutured with sterile surgical silk. Rats were caged individually and examined daily. They were perfused for histological examination at sequential 12 hr intervals from 3 to 5 d after injection (3 d, $n = 11$ rats; 3.5 d, $n = 16$ rats; 4 d, $n = 14$ rats; 4.5 d, $n = 4$ rats; 5 d, $n = 10$ rats). None of the rats exhibited neurological symptoms or behavioral changes at these times, which correspond to the asymptomatic period of rabies (Ugolini, 1995b; Tang et al., 1999). At the chosen time points the rats were anesthetized deeply (Avertin, 2.5 ml/100 gm of body weight) and perfused transcardially with 500 ml of PBS, followed by 500 ml of 4% paraformaldehyde in 0.1 M phosphate buffer and 500 ml of 15% sucrose in 0.1 M phosphate buffer (perfusates, pH 7.4). The brains were dissected out and transferred to a 15% sucrose solution in which they were kept overnight at 4°C for cryoprotection before histological processing.

In five rats the rabies virus injections as above were combined in the same surgical session with ipsilateral spinal injections of the retrograde fluorescent tracer Fluoro-Ruby to identify rubrospinal neurons in the same experiment. For this purpose a hemi-laminectomy was performed to expose the right side of the C3–C5 spinal segments, and two injections (3 μl each) of Fluoro-Ruby 10% were made into the white and gray matter, centered on the dorsolateral funiculus in which the rubrospinal tract is located. These rats were killed for analysis 5 d later.

Histology. Brains were cut on a cryostat in coronal sections (50 μm) that were collected free-floating in four parallel series. In two alternative series the rabies immunolabeling was detected by using the peroxidase–antiperoxidase method (Ugolini, 1995b). One series was counterstained with cresyl violet. Sections from the remaining series were used for dual-color immunofluorescence detection of rabies virus and choline acetyltransferase, for double fluorescence detection of rabies virus and Fluoro-Ruby, or as a positive control in the various immunohistochemical reactions.

For immunoperoxidase staining the free-floating sections were incubated at room temperature in 0.3% H_2O_2 in PBS for 1 hr, followed by 0.2% swine normal serum in PBS for 1 hr, and then were incubated overnight at 4°C with rabbit polyclonal antibodies raised against rabies virus nucleocapsid (dilution, 40 μg/ml; Sanofi Pasteur, Paris, France). Subsequently, the sections were incubated at room temperature for 2 hr in swine anti-rabbit IgG (Dako, Trappes, France) diluted 1:200, followed by 2 hr in rabbit immunoperoxidase complex (Dako) diluted 1:200. Several washes with PBS were performed between steps. Peroxidase activity was revealed by incubation (2–10 min) in a metal-enhanced diaminobenzidine substrate kit (Pierce, Rockford, IL). Staining specificity was checked by incubating each series together with positive controls (i.e., sections from brains having shown rabies immunolabeling in previous reactions) and negative controls (sections from noninfected brains). Sections were mounted on gelatin-coated slides, air-dried, and coverslipped with Entellan (Merck, Whitehouse Station, NJ).

One series of sections from rats killed at 4 d was treated by using a dual-color immunofluorescence protocol for simultaneous detection of rabies virus and choline acetyltransferase, used here as a marker for motoneurons. Free-floating sections were incubated in 0.4% Triton X-100 for 30 min and in 3% donkey serum (Chemicon, Temecula, CA) for 1 hr, followed by incubation (20 hr) at 4°C in a mixture of mouse monoclonal antibodies recognizing the rabies P-protein (Laboratoire de Génétique des Virus, Gif-sur-Yvette, France) diluted 1:100 and goat anti-choline acetyltransferase (Chemicon AB144P) diluted 1:100. After being rinsed in PBS, the sections were incubated for 2 hr at room temperature in a mixture of fluorescein isothiocyanate (FITC)-conjugated donkey anti-mouse IgG (1:100; Jackson ImmunoResearch, West Grove, PA), and indocarbocyanine (Cy3)-conjugated donkey anti-goat IgG (1:100; Chemicon). Primary and secondary antibodies were diluted in PBS containing 3% donkey normal serum and 2% bovine serum albumin. Staining specificity was checked by omitting the primary or secondary antibody and by using positive and negative controls. After several washes in PBS the sections were mounted on slides and coverslipped with Vectashield (Vector Laboratories, Burlingame, CA).

In the experiments involving rabies immunolabeling in combination with retrograde labeling of rubrospinal neurons by means of the red fluorescent tracer Fluoro-Ruby, the sections were treated for immunofluorescent (FITC, green) visualization of the rabies antigen as described above.

Analysis. Fluorescent preparations were observed with a Leitz epifluorescence microscope. Selected images were captured by using a digital camera (Leitz DC-250, Wetzlar, Germany) and the IM-1000 Image Manager (Leica, Nussloch, Germany).

Rabies-immunolabeled neurons in the brain were plotted by using an analog *x–y* plotter connected by potentiometers to the microscope stage or the computer-assisted Neurolucida system (MicroBrightField, Colchester, VT). The location of labeled neurons was illustrated in various drawings. In all drawings the retrogradely labeled orbicularis oculi motoneurons are indicated by asterisks. Each dot represents one rabies transneuronally labeled neuron. The nomenclature is according to Paxinos and Watson (1986).

RESULTS

Kinetics of infection of orbicularis oculi motoneurons (first-order neurons)

After rabies virus injection into the right orbicularis oculi muscle, rabies-immunolabeled motoneurons were found exclusively within the dorsolateral subdivision of the ipsilateral facial nucleus (Fig. 1*A*), where orbicularis oculi motoneurons are known to be located (Martin and Lodge, 1977; Faulkner et al., 1997). Primary sensory neurons in Gasser's ganglion, which also innervate the orbicularis oculi muscle, were not labeled, confirming the lack of peripheral uptake of rabies virus by sensory neurons (Tang et al., 1999; Kelly and Strick, 2000; Graf et al., 2002). At none of the time points that were explored (3–5 d after inoculation) were labeled motoneurons found in other subdivisions of the facial nucleus (Fig. 1*A*), showing that no spurious diffusion of the virus tracer occurred either from the orbicularis oculi muscle to neighboring facial muscles or within the facial nucleus itself.

Rabies-immunolabeled orbicularis oculi motoneurons showed normal size, morphology, and Nissl staining as well as normal levels of expression of the choline acetyltransferase marker. Glial cells were not infected. As illustrated in Figure 1*A*, the number of positive motoneurons quantified at 3 d after inoculation was low (12 ± 4 SD; $n = 8$ animals) and did not show any significant

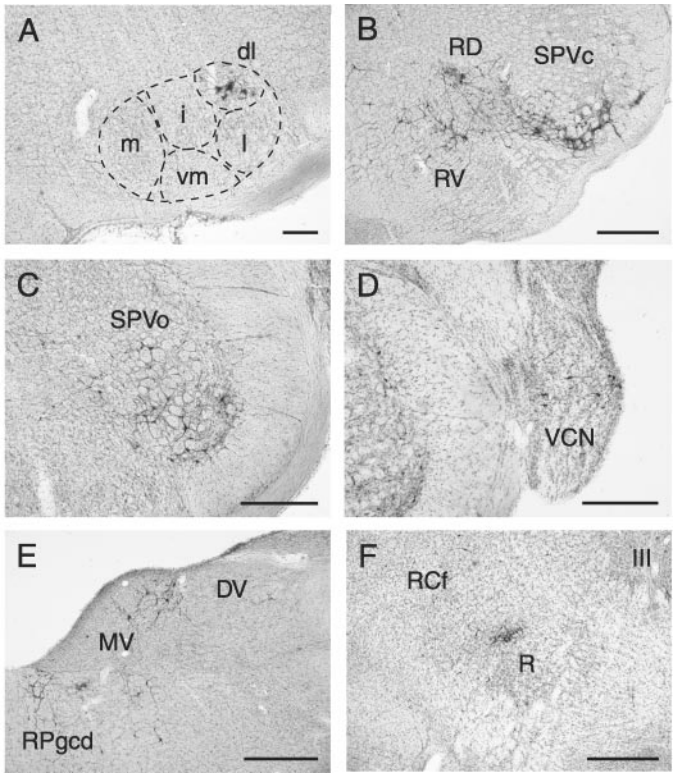

Figure 1. Shown are photomicrographs of rabies-immunolabeled brainstem neurons at 3 d (*A*), 3.5 d (*B, D, F*), and 4 d (*C, E*) after rabies virus injection into the right orbicularis oculi muscle. *A*, Labeled orbicularis oculi motoneurons in the dorsolateral (*dl*) division of the facial nucleus. Note the absence of labeling in the other divisions. *B*, Labeled neurons in the ipsilateral medullary reticular formation. *C*, Labeled neurons in the ipsilateral spinal trigeminal nucleus, pars oralis (*SPVo*). *D*, Labeled neurons in the ipsilateral ventral cochlear nucleus (*VCN*). *E*, Labeled neurons in the ipsilateral medial vestibular nucleus (*MV*) and in the nucleus reticularis paragigantocellularis dorsalis (*RPgcd*). *F*, Labeled neurons in the dorsolateral quadrant of the contralateral red nucleus (*R*) and overlying pararubral area. Scale bars: *A*, 100 μm; *B–F*, 500 μm. *i*, *l*, *m*, *vm*, Intermediate, lateral, medial, and ventromedial divisions of the facial nucleus; *III*, oculomotor nucleus; *DV*, descending vestibular nucleus; *RCf*, nucleus reticularis cuneiformis; *RD*, nucleus reticularis dorsalis; *RV*, nucleus reticularis ventralis, *SPVc*, spinal trigeminal nucleus, pars caudalis.

increase at later time points (13 ± 3; counted from $n = 10$ animals at 5 d). The low number of retrogradely labeled motoneurons is probably attributable to the fact that the tracer injections had involved only a few motor endplates because of their restricted, nonintermingled distribution in the orbicularis oculi muscle. Notably, the finding that labeled orbicularis oculi motoneurons did not become more numerous with time indicates that rabies virus uptake remained restricted to the injection sites, i.e., the virus tracer did not diffuse even within the muscle itself.

Retrograde transneuronal labeling of eyelid premotor networks

The kinetics of retrograde transneuronal transfer of rabies virus was studied at sequential 12 hr intervals from 3 to 5 d after injection. Transneuronal transfer was time-dependent. The results obtained at successive time points were highly reproducible, showing a progressive increase in the number of labeled neural sites and in the number of rabies-immunolabeled neurons. As observed in other rodent models (Ugolini, 1995b; Tang et al., 1999), 3 d after injection was sufficient for the onset of transneuronal labeling of second-order neurons, i.e., neurons projecting monosynaptically onto orbicularis oculi motoneurons. At this time point, however, transneuronal labeling occurred only in some cases and involved only a subset of the total population of second-order neurons, presumably those that are connected more heavily with orbicularis oculi motoneurons and that synapse proximally on the motoneurons soma-dendritic trees (Ugolini, 1995b; Graf et al., 2002). Thus, only a few labeled neurons were found in specific portions of the brainstem reticular formation (nuclei reticularis ventralis, dorsalis, magnocellularis, and cuneiformis) and auditory (periolivary) structures (see below) and at the ventral border of the spinal trigeminal nucleus in some cases.

At 3.5 d, transneuronally labeled neurons at these locations became more numerous, and additional sites became labeled (Fig. 2). On the basis of the correspondence with the results of tracing studies (Courville, 1966; Takeuchi et al., 1979; Hinrichsen and Watson, 1983; Travers and Norgren, 1983; Takada et al., 1984; Holstege et al., 1986a,b; Isokawa-Akesson and Komisaruk, 1987; Fort et al., 1989), neuronal labeling at this time point still involved second-order neurons (Ugolini, 1995b). Notably, only a few labeled neurons were seen within the medial border of the ipsilateral spinal trigeminal nucleus, pars spinalis, interpolaris, and oralis (Fig. 2). Most of the labeled neurons were located ipsilaterally in specific portions of the caudal medullary lateral reticular formation (labeled already at 3 d), i.e., in the nucleus reticularis dorsalis and in the ventral part of the caudalmost portion of the nucleus reticularis parvocellularis as well as in the adjoining nucleus reticularis ventralis (Figs. 1*B*, 2*B–D*). Contralaterally, labeling in the reticular formation at these levels was sparse and located mainly ventrally in the nucleus reticularis ventralis and parvocellularis (Fig. 2*B–D*). More rostral portions of the medullary lateral reticular formation showed very little labeling. In the medullary medial reticular formation the labeling involved primarily the nucleus reticularis magnocellularis bilaterally, mainly ipsilaterally (Fig. 2*E–G*). A few labeled neurons also were found in the nucleus reticularis gigantocellularis, in the medial part of the nucleus reticularis paragigantocellularis dorsalis, and in the adjoining medial longitudinal fasciculus. More rostrally, some labeled neurons were seen in the nucleus reticularis pontis caudalis and oralis, particularly in the ventral reticular area neighboring the superior olivary complex. Notably, a dense accumulation of labeled neurons was found, mainly ipsilaterally, in auditory structures in which labeling already had been observed 12 hr previously, particularly in the caudal periolivary nuclei, in the nucleus of the trapezoid body and the ventral periolivary nucleus, and, to a lesser degree, in the rostral periolivary nucleus (Fig. 2*H–J*). Labeling also occurred bilaterally in the caudal part of the ventral cochlear nucleus (Figs. 1*D*, 2*F*). A dense accumulation of labeled neurons was seen in the nucleus of Kölliker–Fuse and ventral parabrachial nuclei ipsilaterally (Fig. 2*J*). Sparse labeling was found in the nucleus of the solitary tract in only two (of 16) cases. A few labeled neurons were seen in the medial vestibular nucleus at rostral levels (Fig. 2). Notably, dense labeling at this time point appeared in specific portions of the deep cerebellar nuclei, i.e., in the caudolateral part of the anterior interpositus nucleus and dorsolateral hump ipsilaterally (Fig. 2*G*). In the mesencephalon a dense accumulation of labeled neurons was seen in the dorsolateral quadrant of the contralateral red nucleus and in the dorsally adjoining pararubral area (Ruigrok and Cella, 1995), which is part of the nucleus reticularis cuneiformis (Figs. 1*F*, 2*K,L*), suggesting strong synaptic links with orbicularis oculi motoneurons. Sparse labeling occurred in the interstitial nucleus

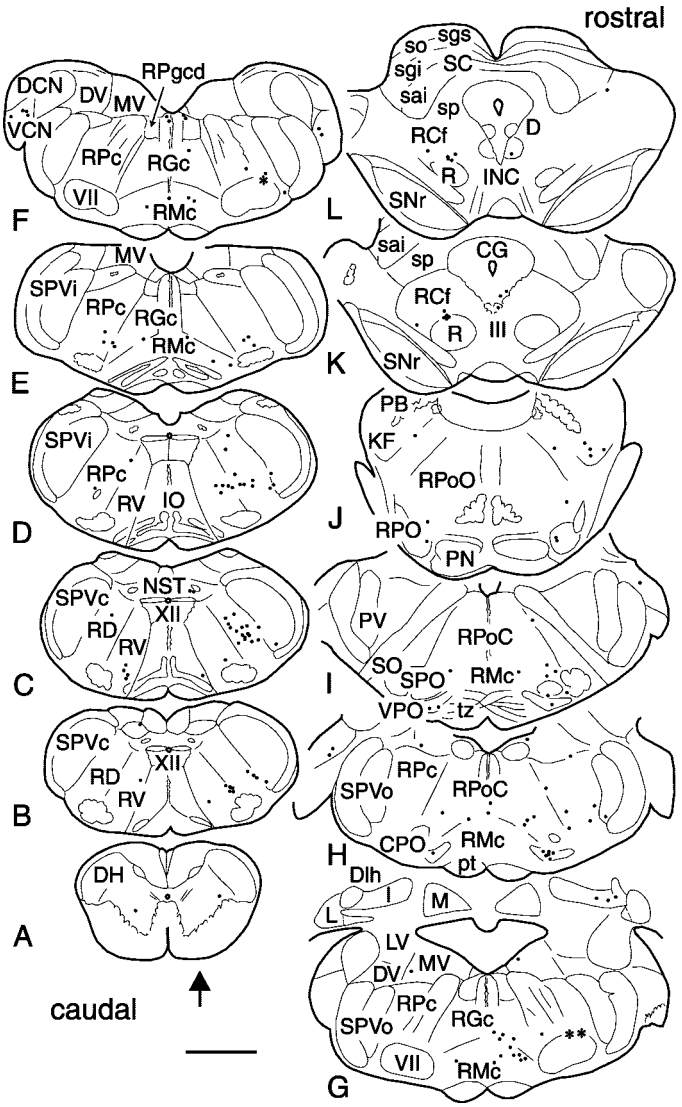

Figure 2. Brainstem distribution of rabies-immunolabeled neurons at 3.5 d after rabies virus injection into the right orbicularis oculi muscle. *A–L*, Labeled sections are arranged caudorostrally. The *arrows* indicate the side that is ipsilateral to the injection. *Asterisks* in *F, G*, Retrogradely labeled orbicularis oculi motoneurons in the dorsolateral division of the facial (*VII*) nucleus. Each *dot* represents one labeled neuron. Scale bar, 2 mm. *CG*, Central gray; *CPO*, caudal periolivary nucleus; *D*, nucleus of Darkschewitsch; *DCN*, dorsal cochlear nucleus; *Dlh*, dorsolateral hump; *DH*, dorsal horn; *DV*, descending vestibular nucleus; *I*, interpositus nucleus; *INC*, interstitial nucleus of Cajal; *IO*, inferior olive; *KF*, Kölliker–Fuse nucleus; *L*, lateral (dentate) nucleus; *LV*, lateral vestibular nucleus; *M*, medial (fastigial) nucleus; *MV*, medial vestibular nucleus; *NST*, nucleus of the solitary tract; *PB*, parabrachial nucleus; *PT*, pyramidal tract; *PV*, principal trigeminal nucleus; *R*, red nucleus; *RCf*, nucleus reticularis cuneiformis; *RD*, nucleus reticularis dorsalis; *RGc*, nucleus reticularis gigantocellularis; *RMc*, nucleus reticularis magnocellularis; *RPc*, nucleus reticularis parvocellularis; *RPgcd*, nucleus reticularis paragigantocellularis dorsalis; *RPO*, rostral periolivary region; *RPoC*, nucleus reticularis pontis caudalis; *RPoO*, nucleus reticularis pontis oralis; *RSc*, nucleus reticularis subceruleus; *RV*, nucleus reticularis ventralis; *sai*, stratum album intermedialis; *SC*, superior colliculus; *sgi*, stratum griseum intermedialis; *sgs*, stratum griseum superficialis; *SNr*, substantia nigra pars reticulata; *so*, stratum opticum; *SO*, superior olive; *sp*, strata profunda; *SPO*, superior paraolivary nucleus; *SPVc, SPVi, SPVo*, spinal trigeminal nuclei, pars caudalis, interpolaris, and oralis; *tz*, trapezoid body; *VCN*, ventral cochlear nucleus; *VPO*, ventral periolivary nucleus; *III*, oculomotor nucleus; *XII*, hypoglossal nucleus.

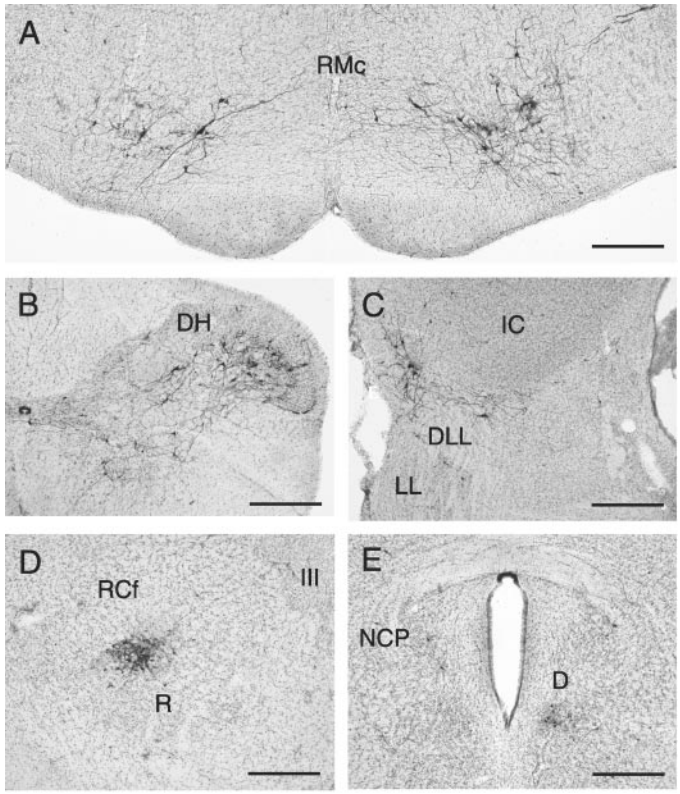

Figure 3. Rabies-immunolabeled neurons at 4 d after rabies virus injection into the right orbicularis oculi muscle. *A*, Transneuronally labeled neurons in nucleus reticularis magnocellularis (*RMc*). *B*, Labeled neurons in the ipsilateral dorsal horn (*DH*) and intermediate zone of the upper cervical cord. *C*, Labeled neurons in the contralateral dorsal nucleus of the lateral lemniscus (*DLL*) and inferior colliculus (*IC*). *D*, Labeled neurons in the dorsolateral quadrant of the contralateral red nucleus (*R*) and overlying pararubral area at 4 d (see also 3.5 d) (Fig. 1*F*). *E*, Labeled neurons in the nucleus of Darkschewitsch (*D*) and nucleus of the posterior commissure (*NCP*). Scale bars, 500 μm. *III*, Oculomotor nucleus; *LL*, lateral lemniscus.

of Cajal (Fig. 2*L*). Some labeled neurons also were found consistently within the ipsilateral oculomotor nucleus and in the dorsally adjoining supraoculomotor area (Fig. 2*K*). The neurons labeled within the oculomotor nucleus appeared to be smaller than motoneurons. They were identified clearly as oculomotor internuclear neurons and not motoneurons because they were not cholinergic, as shown by the results of dual-color immunofluorescence for simultaneous visualization of rabies and choline acetyltransferase antigens (see below).

A great increase in the distribution and number of labeled neurons occurred at 4 d after inoculation. This additional 12 hr interval is consistent with an additional synaptic step of transfer (Ugolini, 1995b; Tang et al., 1999; Graf et al., 2002). Correspondingly, transneuronal labeling obtained at this time point clearly involved higher order (presumably third-order) neurons connected polysynaptically to orbicularis oculi motoneurons.

The distribution of labeling in the medulla, pons, and mesencephalon at 4 d is illustrated in Figures 3-5. At medullary levels one of the characteristic features of this time point was the appearance of extensive labeling ipsilaterally in the principal and spinal trigeminal nuclei and in the dorsal horn of the first cervical segments (Figs. 1*C*, 3*B*, 4). Labeling was particularly dense and widely distributed in deep layers of the dorsal horn (Figs. 3*B*, 4*A*)

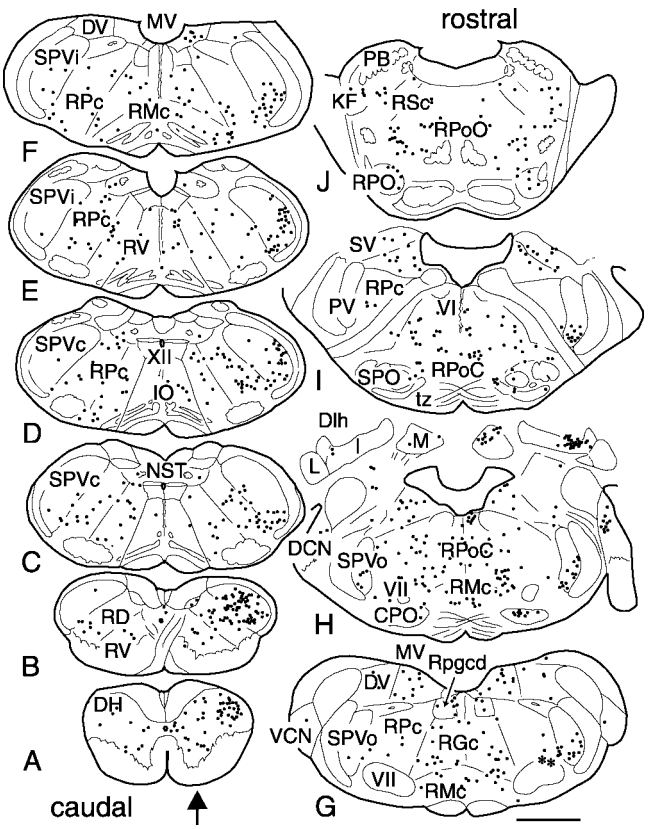

Figure 4. Distribution of rabies-immunolabeled neurons in the medulla and pons at 4 d after rabies virus injection into the right orbicularis oculi muscle. *A–J*, Labeled sections are arranged caudorostrally. *Arrows* indicate the side that is ipsilateral to the injected muscle. *Asterisks* in *G*, Retrogradely labeled orbicularis oculi motoneurons in the dorsolateral division of the facial (*VII*) nucleus. Each *dot* represents one labeled neuron. Scale bar, 2 mm. For abbreviations see the legend of Figure 2.

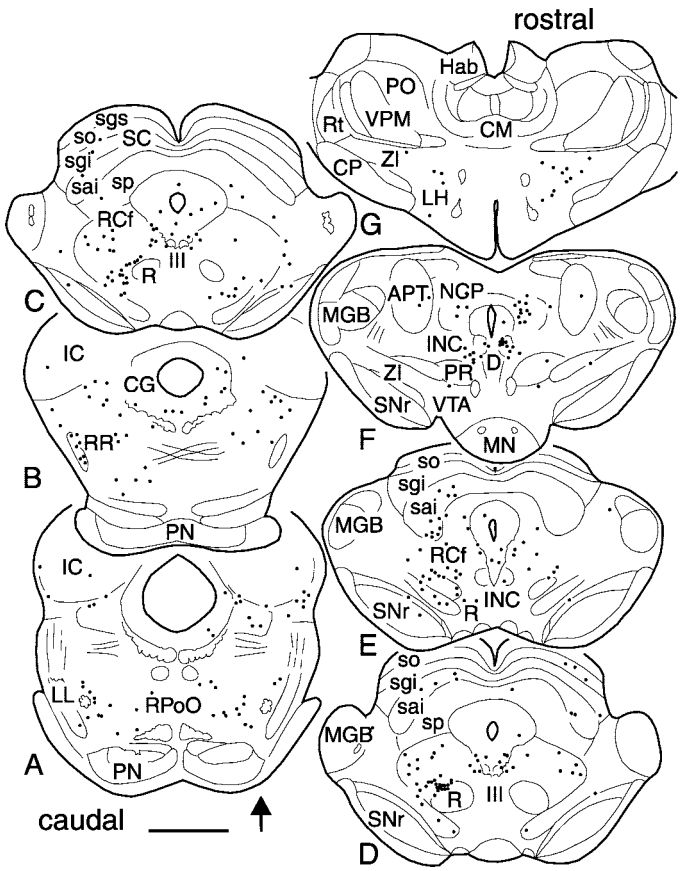

Figure 5. Distribution of rabies-immunolabeled neurons in the mesencephalon and caudal diencephalon at 4 d after rabies virus injection into the right orbicularis oculi muscle. *A–G*, Labeled sections are arranged caudorostrally. *Arrows* indicate the side that is ipsilateral to the injected muscle. Each *dot* represents one labeled neuron. Scale bar, 2 mm. For abbreviations see the legend of Figure 2. *APT*, Anterior pretectal nucleus; *CM*, central medial nucleus; *CP*, cerebral peduncle; *Hab*, habenula; *IC*, inferior colliculus, *LH*, lateral hypothalamus; *LL*, lateral lemniscus, *MGB*, medial geniculate body; *MN*, mamillary nuclei; *NCP*, nucleus of the posterior commissure; *PN*, pontine nuclei; *PO*, posterior thalamic nucleus; *PR*, prerubral field; *RR*, retrorubral nucleus; *Rt*, reticular thalamic nucleus; *VPM*, ventral posteromedial thalamic nucleus; *VTA*, ventral tegmental area; *ZI*, zona incerta.

and in the adjoining caudalmost portion of the spinal trigeminal nucleus, pars caudalis (Fig. 4*B*). At more rostral levels of the ipsilateral spinal trigeminal nucleus (pars caudalis, interpolaris, and oralis) and in the principal trigeminal nucleus, labeled neurons were seen only in the ventral part of these nuclei (Figs. 1*C*, 4*C–I*). Only sparse labeling was found in the contralateral spinal trigeminal nuclei and dorsal horn (Fig. 4).

A considerable increase in the number and distribution of labeled neurons occurred also in the medullary and pontine reticular formation, where labeling became much more bilateral but still showed a clear dominance ipsilaterally in the portions of the nuclei reticularis dorsalis, ventralis, and parvocellularis that already had shown labeling at previous time points (Fig. 4). The increase in areal distribution of reticular neurons was particularly noticeable in the intermediate zone of the upper cervical segments, in the nucleus reticularis gigantocellularis, reticularis pontis caudalis and oralis, and reticularis cuneiformis (Fig. 4). Rabies immunolabeling provided a complete visualization of neuronal morphology, including distal dendrites (Fig. 3*A*).

Another feature of the 4 d time point was the dense labeling bilaterally in the medial, descending, and superior vestibular nuclei, particularly in the medial vestibular nucleus (Figs. 1*E*, 4*F–I*). Labeling of the parabrachial nuclei became more pronounced and bilateral, and some labeling occurred consistently in the nucleus of the solitary tract (Fig. 4*C,D*).

Besides a moderate increase in the number of labeled neurons in the auditory structures labeled at previous time points, additional labeling appeared bilaterally in the dorsal cochlear nucleus (Fig. 4*H*), in external layers of the inferior colliculus, and in the area ventral to it corresponding to the dorsal nucleus of the lateral lemniscus (Figs. 3*C*, 5*A,B*). Sparse labeling occurred also in more ventral portions of the nucleus of the lateral lemniscus.

In the contralateral red nucleus the labeled neurons increased in number but remained restricted to the dorsolateral quadrant of the red nucleus and the adjoining pararubral area (Figs. 3*D*, 5*C,D*). The contralateral prerubral and retrorubral areas also were labeled densely (Fig. 5).

At 4 d, labeling also appeared in intermediate and deep layers of the superior colliculus, mainly contralaterally (Fig. 5*C–E*). Several mesencephalic oculomotor-related structures were labeled, such as the nucleus of Darkschewitsch, the interstitial nucleus of Cajal, and the nucleus of the posterior commissure (Fig. 3*E*), mainly ipsilaterally, the supraoculomotor area, and some internuclear interneurons located inside the oculomotor complex (Fig. 5*C–F*). Besides the supraoculomotor area, labeling

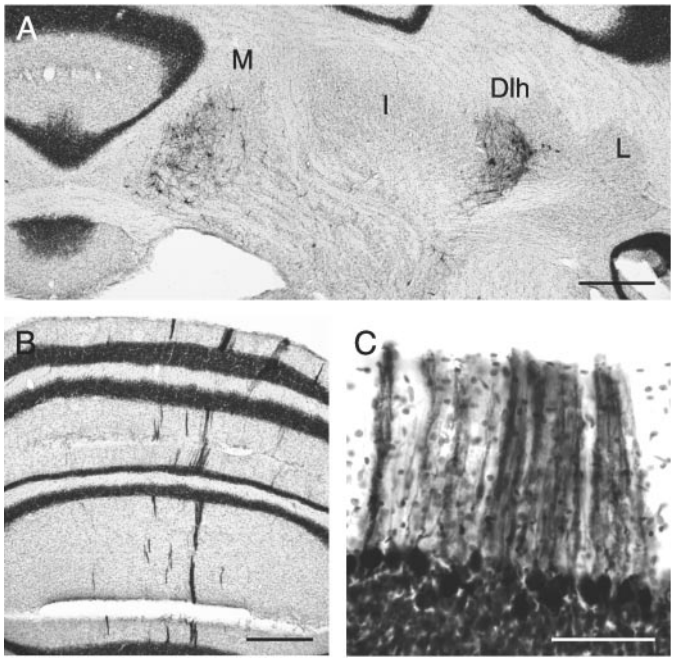

Figure 6. Rabies-immunolabeled neurons in the cerebellar cortex and nuclei. *A*, Transneuronally labeled neurons in the medial (*M*, fastigial) nucleus, interpositus (*I*) nucleus, and dorsolateral hump (*Dlh*) at 4 d after the injection of rabies virus into the ipsilateral orbicularis oculi muscle. *B*, Transneuronal labeling of higher order neurons in the cerebellar vermis at 5 d after injection. Note the zonal distribution of labeled Purkinje cells. *C*, Coronal section through the paravermis, illustrating another area in which rabies-immunolabeled Purkinje cells were observed at 5 d after rabies virus injection in the ipsilateral orbicularis oculi muscle. Scale bars: *A*, *B*, 500 μm; *C*, 150 μm.

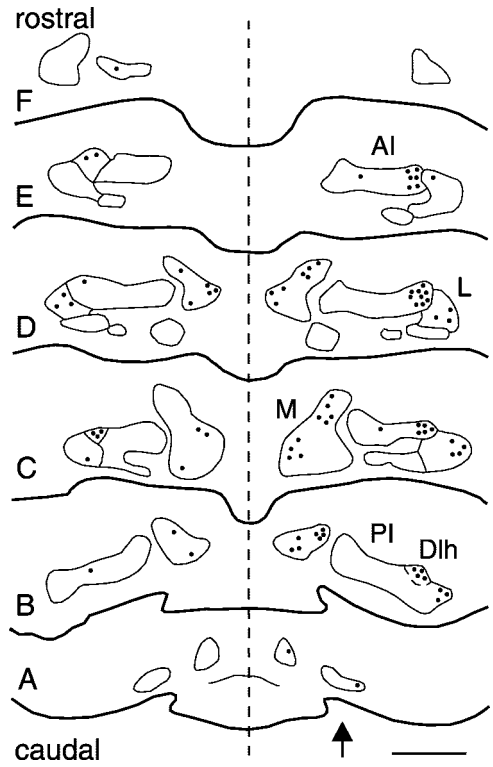

Figure 7. Distribution of rabies-immunolabeled neurons in the deep cerebellar nuclei at 4 d after rabies virus injection into the right orbicularis oculi muscle (*arrow* indicates ipsilateral side). Sections in *A–F* are arranged from caudal to rostral. The *dashed line* denotes the midline. Each *dot* represents one labeled neuron. Note transneuronally labeled neurons bilaterally, with clear ipsilateral dominance, in medial (*M*, fastigial) nucleus, dorsolateral hump (*Dlh*), lateral part of posterior interpositus (*PI*) and anterior interpositus (*AI*), and lateral (*L*, dentate) nuclei. Scale bar, 2 mm.

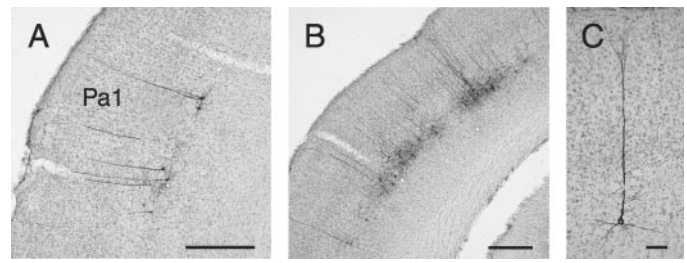

Figure 8. Photomicrographs illustrating transneuronally labeled pyramidal cells in the contralateral parietal cortex at 4–5 d after rabies virus injection into the right orbicularis oculi muscle. *A*, Coronal section of the parietal cortex, area 1 (*Pa1*) at 4 d. *B*, Parietal cortex, area 1, at 5 d. Note the increase in the number of rabies-immunolabeled pyramidal cells. *C*, High-power photomicrograph of parietal cortex at 4.5 d. Note Golgi-like labeling of a pyramidal cell in layer V. Scale bars: *A*, *B*, 500 μm; *C*, 100 μm.

involved more dorsal portions of the central gray and the dorsal raphe nucleus (Fig. 5*B–D*). Some labeling also was seen in the pretectal nuclei (Fig. 5*F*). Because the pretectal area receives afferences from the retina (Holstege et al., 1986a,b), this pathway is potentially involved in flash-evoked blinks (Evinger et al., 1991; Gruart et al., 1995). Some labeling also was found bilaterally in the substantia nigra, lateral hypothalamus, and zona incerta (Fig. 5*E–G*).

In the deep cerebellar nuclei (Figs. 4*H*, 6*A*, 7), dense labeling occurred in the dorsolateral hump and in the lateral part of the anterior interpositus nucleus and posterior interpositus nucleus, except its caudalmost portion (Figs. 4*H*, 6*A*, 7*B–E*). Labeling was bilateral with a clear ipsilateral dominance (contralateral labeling involving mainly the dorsolateral hump) (Fig. 7*C*). Bilateral labeling with a clear ipsilateral dominance appeared also in the medial (fastigial) nucleus and in the lateral (dentate) nucleus (Figs. 4*H*, 6*A*, 7*B–E*).

Another distinctive feature of the 4 d time point was the appearance of labeling in the cerebral cortex (Figs. 8*C*, 9), which is a clear reflection of polysynaptic links with orbicularis oculi motoneurons. Labeling involved exclusively pyramidal neurons in layer V (see example in Fig. 8*A*). Most of the labeled neurons were located in parietal cortex areas 1 and 2 (Pa1 and Pa2; Paxinos and Watson, 1986) bilaterally, with a clear contralateral dominance (Fig. 9). A few labeled neurons also were located in frontal (F1, F2) and occipital (Oc2L) cortices contralaterally. In four (of 14) animals some labeled pyramidal cells also were found in the perirhinal and temporal (Te1) cortices (data not shown).

Data collected at 4.5 and 5 d were characterized by an increase in the number of labeled interneurons in trigeminal, vestibular, auditory, and oculomotor-related structures as well as in the reticular formation plus labeling at some additional sites, for example some neurons within the lateral vestibular nucleus. Even at these time points the specificity of transfer was illustrated by the lack of invasion of brainstem sites that clearly are unrelated to eyelid motoneurons, such as other brainstem motor nuclei (hypoglossus, abducens, ambiguous, etc.).

A noticeable increase in the number of labeled structures

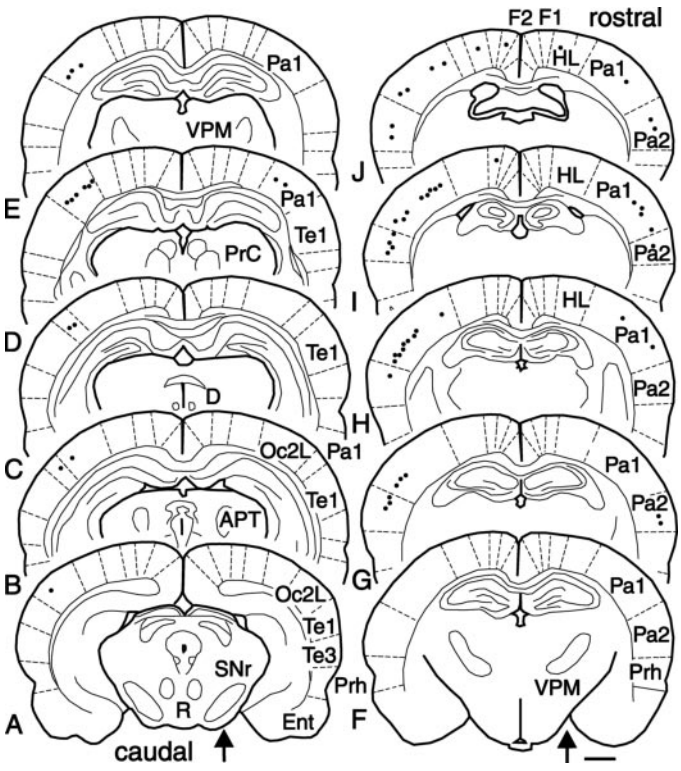

Figure 9. Distribution of rabies-immunolabeled neurons in the cerebral cortex at 4 d after rabies virus injection into the right orbicularis oculi muscle. *A–J*, Labeled sections are arranged from caudal to rostral. *Arrows* indicate the ipsilateral side. Each *dot* represents one labeled neuron. Scale bar, 2 mm. At 4 d the labeled neurons were concentrated in parietal cortex, areas 1 and 2 (*Pa1* and *Pa2*) bilaterally, with a clear contralateral dominance. *APT*, Anterior pretectal area; *CG*, central gray; *D*, nucleus of Darkschewitsch; *Ent*, entorhinal cortex; *F1*, frontal cortex, area 1; *F2*, frontal cortex, area 2; *HL*, hindlimb area of parietal cortex; *INC*, interstitial nucleus of Cajal; *Oc2L*, occipital cortex area 2, lateral; *PrC*, precommissural nucleus; *Prh*, perirhinal cortex; *R*, red nucleus; *SNr*, substantia nigra, pars reticulata; *Te1*, temporal cortex, area 1; *Te3*, temporal cortex, area 3; *VPM*, ventral posteromedial thalamic nucleus.

occurred at diencephalic levels. In the hypothalamus the labeling appeared in the anterior hypothalamus and the dorsomedial hypothalamic nuclei, besides the lateral hypothalamic area, already labeled at 4 d. The ventral posteromedial and the posterior thalamic nuclei showed some labeling bilaterally, presumably via their connections to the labeled cortical areas. Labeling in the cerebral cortex became more extensive. As illustrated in Figure 8, *B* and *C*, the number of labeled cells in the parietal cortex showed a great increase (>300%) compared with that obtained at 4 d (Fig. 8*B*), and the labeling of individual pyramidal neurons in layer V became Golgi-like (Fig. 8*C*, compare with *B*). Both parietal areas Pa1 and Pa2 (Paxinos and Watson, 1986) were heavily labeled bilaterally, still with a contralateral dominance. Labeling also occurred consistently in some portions of temporal (Te1 and Te3) and Oc2L cortices contralaterally and in frontal (F1 and F2 areas) and perirhinal cortices bilaterally, whereas no labeling was found in entorhinal cortex or hippocampus.

In the cerebellum (Fig. 6*B,C*) the labeling appeared in vermal and paravermal (c_1–c_3 areas) Purkinje cells (for references, see Gruart et al., 1997). The labeled Purkinje cells showed a clear zonal organization, being arranged in narrow rostrocaudal bands (Fig. 6*B,C*).

Identification of oculomotor internuclear neurons projecting to orbicularis oculi motoneurons

Some rabies-immunolabeled neurons were found in the oculomotor nucleus, mainly ipsilaterally, in all cases from 3.5 d onward (monosynaptic time point). Their number and distribution did not increase substantially with time. To clarify whether they were interneurons or motoneurons, we treated sections through the oculomotor nuclei with a dual-color immunofluorescence protocol for simultaneous visualization of rabies and choline acetyltransferase. Sections through the facial nucleus, containing rabies-immunolabeled orbicularis oculi motoneurons, were reacted together as positive controls. Choline acetyltransferase is an excellent motoneuron marker, and we have shown previously that rabies-infected motoneurons are able to express choline acetyltransferase antigen at normal levels (Tang et al., 1999; Graf et al., 2002). The results showed unequivocally that rabies-immunolabeled neurons in the oculomotor nucleus are interneurons (and not motoneurons), because they are not cholinergic (Fig. 10). The possibility of false negative results for colocalization of rabies and choline acetyltransferase antigen in motoneurons clearly can be ruled out in view of the positive expression of the choline acetyltransferase antigen in rabies-infected orbicularis oculi motoneurons in the same experiments.

Specificity of rubral projection to orbicularis oculi motoneurons

Until now, it was unknown whether the rubral projections to the facial nucleus are mediated by separate rubral population or are axon collaterals of rubrospinal-projecting neurons (Mizuno and Nakamura, 1971). To clarify this issue, retrograde transneuronal labeling with rabies virus of the rubral neurons innervating orbicularis oculi motoneurons was combined in the same experiments with conventional (single-step) retrograde labeling of rubrospinal neurons by using Fluoro-Ruby. As expected, the injections of Fluoro-Ruby into the rubrospinal tract at upper cervical levels resulted in comprehensive labeling of rubrospinal neurons, as shown by their widespread distribution in all spinal-projecting portions of the red nucleus, including its lateral horn (Fig. 11*A,C*) (Huisman et al., 1981; Strominger et al., 1987; Ugolini, 1992; Tang et al., 1999). In contrast, the transneuronally labeled rubrofacial neurons occupied exclusively the dorsolateral quadrant of the red nucleus and the dorsally adjoining pararubral area (Fig. 11*B,D*). Our results (Fig. 11) show that rubrofacial neurons innervating orbicularis oculi motoneurons monosynaptically and disynaptically are clearly a separate population from the rubrospinal-projecting ones. Despite the topographical overlap between the two populations in the dorsolateral quadrant, we found only a very small percentage (2%) of double-labeled neurons projecting with axon collaterals to both targets (Fig. 11*C,D*, *arrows*). This has negligible functional significance, if any, considering also that the projections from the red nucleus to functionally different targets generally are more collateralized in the rat than in other mammals (cat and monkey) (Huisman et al., 1981, 1982).

DISCUSSION

General remarks

Neuronal networks involved in the generation and control of spontaneous, reflex, and learned eyelid responses were revealed here by transneuronal transfer of rabies virus from the orbicularis oculi muscle. Because of its highly specific propagation by retrograde transneuronal transfer across an unlimited number of syn-

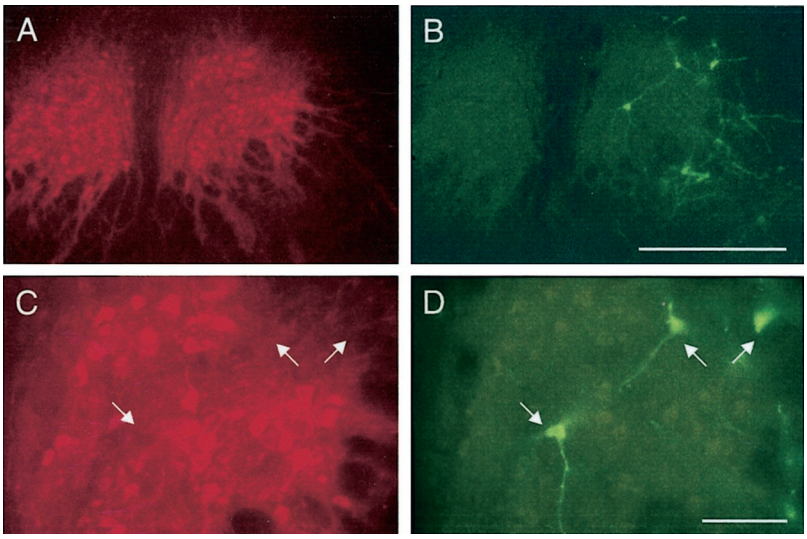

Figure 10. Dual-color immunofluorescence for choline acetyltransferase (a motoneuron marker; *A, C*) and rabies virus (*B, D*) in the oculomotor nucleus at 4 d after the injection of rabies virus into the right orbicularis oculi muscle. *A*, *C*, Motoneurons in the oculomotor nucleus, identified by their expression of choline acetyltransferase (Cy3; *red*). *B*, *D*, Rabies-immunolabeled neurons (FITC; *green*) in the ipsilateral oculomotor nucleus in the same sections. They are identified here as interneurons and not motoneurons, because they are not positive for choline acetyltransferase (*arrows* in *C* point to the empty spaces corresponding to the rabies-immunolabeled neurons shown in *D)*. Scale bars: *A*, *B*, 500 μm; *C*, *D*, 100 μm.

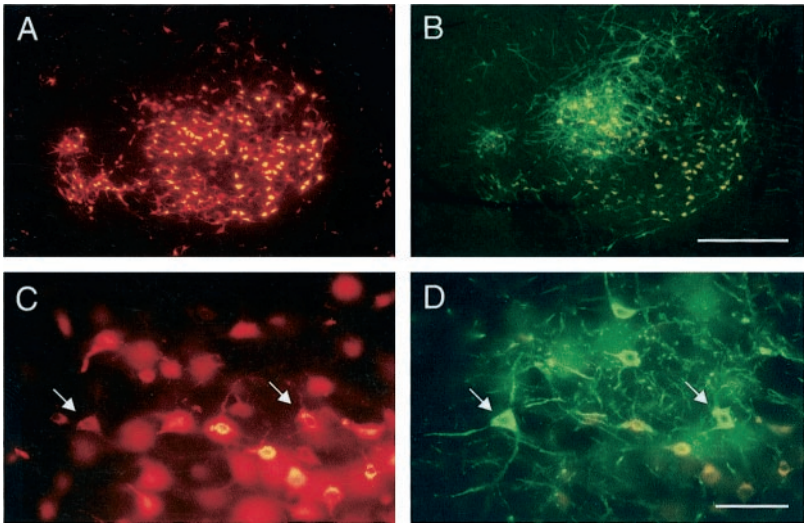

Figure 11. Rubrospinal neurons, labeled retrogradely after injections of Fluoro-Ruby into the right rubrospinal tract in the upper cervical spinal segments (*A, C*), and orbicularis oculi-related rubrobulbar neurons in the same section, labeled by retrograde transneuronal transfer of rabies virus from the right orbicularis oculi muscle (*B, D*). The photomicrographs illustrate the contralateral (*left*) magnocellular red nucleus at 5 d. *A*, Rubrospinal neurons (Fluoro-Ruby; *red*). Note their widespread distribution in all spinal-projecting portions of the red nucleus, including its lateral horn (*left*). *B*, Orbicularis oculi-related rubrofacial neurons (rabies immunolabeling, FITC; *green*). Note their exclusive location in the dorsolateral quadrant of the red nucleus. Note well that the *orange spots* are tissue autofluorescence, inevitably shining through the fluorescence filters. *C*, *D*, High-power view of the dorsolateral quadrant of the red nucleus from *A* and *B*. Despite their extensive overlap, rubrospinal and rubrofacial neurons are two separate populations. *Arrows* in *C* and *D* point to rare examples of double-labeled neurons (projecting with axon collaterals to orbicularis oculi motoneurons and to the spinal cord). Scale bars: *A, B*, 500 μm; *C, D*, 100 μm.

apses (Ugolini, 1995b; Tang et al., 1999; Kelly and Strick, 2000; Graf et al., 2002), the rabies virus tracer represents a formidable step forward compared with previous attempts to map such networks with conventional tracers (Takeuchi et al., 1979; Hinrichsen and Watson, 1983; Holstege et al., 1984, 1986a,b; Takada et al., 1984; Fort et al., 1989; Travers, 1995), which could help to locate putative sources of monosynaptic input to orbicularis oculi motoneurons, but not higher order relays. Virus uptake involved exclusively orbicularis oculi motoneurons in the dorsolateral facial nucleus division (Martin and Lodge, 1977; Faulkner et al., 1997). Infected motoneurons remained viable and did not become more numerous or more widely distributed with time, showing that rabies virus did not diffuse either within the muscle or within the facial nucleus. Transneuronal transfer was time-dependent. The observation that all known sources of monosynaptic input to orbicularis oculi motoneurons were labeled at 3.5 d confirms that the efficacy of transfer of rabies virus is not dependent on transmitter types (Ugolini, 1995b; Graf et al., 2002). However, second-order neurons that synapse proximally on the motoneurons soma-dendritic tree may be visualized earlier than neurons establishing more distal or weaker synaptic contacts (Ugolini, 1995b; Graf et al., 2002).

The results highlight the reflex pathways by which sensory inputs of trigeminal, auditory, vestibular, and visual origins can evoke eyelid responses and the participation of reticular, rubral, cerebellar, and cortical neurons to eyelid control. Potential sites of interactions between networks controlling eye and eyelid movements also are revealed here. Based on our results and as pointed out previously (Holstege et al., 1986a,b; Bracha and Bloedel, 1996), multiple pathways (with coinciding nodal points for different sensory modalities) are available in the eyelid premotor system as putative memory storage sites for classical conditioning of eyelid responses, a widely used model for associative motor learning (Gormezano et al., 1983; Woody, 1986; Thompson and Krupa, 1994).

Sensory modalities to orbicularis oculi motoneurons

Projections to orbicularis oculi motoneurons from the ipsilateral trigeminal nuclei (Erzurumlu and Killackey, 1979; Holstege et al., 1986a, 1988; Pellegrini et al., 1995; Van Ham and Yeo, 1996) mediate the R1 component of the blink reflex (Hiraoka and Shimamura, 1977). Such projections, visualized here at 3–3.5 d, were not substantial. Extensive neuronal labeling in the ipsilateral principal and spinal trigeminal nuclei and upper cervical dorsal horn appeared later (4 d), compatible with additional synaptic steps. The labeled sites receive trigeminal afferents of corneal and

periocular origin (Panneton and Burton, 1981; Pellegrini et al., 1995). Polysynaptic trigeminal afferents to orbicularis oculi motoneurons mediate the R2 blink reflex component via reticular formation and dorsal horn synaptic relays (Hiraoka and Shimamura, 1977; Pellegrini et al., 1995).

Auditory pathways were already labeled heavily at monosynaptic time points, an unexpected result according to the paucity of tone-evoked reflex blinks in rabbits and cats (Gruart et al., 1995, 2000a). A likely explanation is that the rat presents a noticeable startle response. Our results indicate that the underlying connections are derived from the nucleus of the trapezoid body; the caudal, ventral, and rostral periolivary nuclei and neighboring portions of the nucleus reticularis pontis caudalis and oralis (López et al., 1999; Sinex et al., 2001); and the caudal part of the ventral cochlear nuclei bilaterally, mainly ipsilaterally. Higher order neurons are located in the dorsal cochlear nucleus, lateral lemniscus nuclei, and inferior colliculus.

Monosynaptic and disynaptic excitatory and inhibitory potentials have been evoked in facial motoneurons by stimulation of the medial and superior vestibular nuclei (Shaw and Baker, 1983). Our results reveal a few monosynaptic and numerous polysynaptic vestibular afferents (from the medial, superior, and descending vestibular nuclei) to orbicularis oculi motoneurons. Such pathways may be involved in eye–eyelid coordination, for example to prevent blinking during vestibulo-ocular reflex performance.

Visual information involved in light-evoked blinks reaches orbicularis oculi motoneurons via the olivary pretectal nucleus and related mesencephalic structures (Itoh et al., 1983), as confirmed here. Although both orbicularis oculi and accessory abducens motoneurons receive such visual input in the cat (Holstege et al., 1986a,b), only orbicularis oculi motoneurons are able to fire to flashlight presentation in alert behaving animals. Visual afferents to accessory abducens motoneurons are an example of "silent" pathways (Delgado-García et al., 1988; Delgado-García, 1998).

Reticular formation and limbic brainstem afferents

Our results show that specific areas of the medullary, pontine, and mesencephalic reticular formations project onto orbicularis oculi motoneurons. Particularly, ipsilateral projections have substantial monosynaptic (and polysynaptic) components. From our results, these reticular areas are connected more heavily with orbicularis oculi motoneurons than are the trigeminal nuclei. Reticular neurons in such areas that project to the orbicularis oculi division are activated by ipsilateral supraorbital nerve stimulation (Inagaki et al., 1989). Bilateral reticular projections to orbicularis oculi motoneurons explain the bilateral blinks (R2 component; Kugelberg, 1952) evoked by unilateral electrical stimulation of the supraorbital nerve (Pellegrini et al., 1995). They also may explain why eyelid classically conditioned responses present a (weaker) component contralateral to the side of the unconditioned stimulus presentation (Gruart et al., 1995).

The different reticular nuclei probably are involved in the generation and/or integration of commands of different origin (motor cortex, basal ganglia, limbic system). Based on *in vitro* effects of acetylcholine on facial motoneurons (Magariños-Ascone et al., 1999), it may be proposed, for instance, that cholinergic neurons in the dorsal medullary reticular formation, near the hypoglossal nucleus, are involved in the generation of orbicularis oculi motoneuron tonic firing, which is characteristic of R2 responses, eyelid-friendly displays, and classically conditioned responses (Holstege et al., 1986a,b; Fort et al., 1989; Travers, 1995; Trigo et al., 1999).

Some of the identified pathways, such as those derived from the parabrachial and Kölliker–Fuse nuclei, may be involved in the genesis of premotor signals related to the expression of internal emotional states, because limbic structures project to these nuclei through the central amygdala and hypothalamus. Such pathways are not affected by lesions of the pyramidal fibers, explaining the possibility of emotional expression in the absence of voluntary eyelid responses (Holstege et al., 1986a,b).

Eye muscles–eyelid premotor relationships

As shown here, structures belonging to eye movement networks (oculomotor internuclear neurons, supraoculomotor area, interstitial nucleus of Cajal, nucleus of Darkschewitsch, superior colliculus) also innervate monosynaptically or polysynaptically the orbicularis oculi motoneurons. This common network is likely to be involved in coordination of eyelid and eye movements during blink (Bour et al., 2000), intentional saccades, and fast phases of the vestibulo-ocular and optokinetic reflexes, mostly for eye movements in the vertical plane. No labeling occurred in the prepositus hypoglossi nucleus, which is involved in horizontal eye movements. Projections to facial motoneurons from these structures were reported in tracing studies (Takeuchi et al., 1979; Hinrichsen and Watson, 1983; Takada et al., 1984; Holstege et al., 1986a; Isokawa-Akesson and Komisaruk, 1987; Fort et al., 1989) and electrophysiological experiments (Fanardjian and Manvelyan, 1987b; Vidal et al., 1988; May et al., 1990).

Red nucleus and cerebellum

Our results indicate that eyelid-related rubrofacial neurons are clustered in the dorsolateral quadrant of the contralateral red nucleus and pararubral area. As shown here, eyelid-related rubrofacial pathways are clearly independent (i.e., not a collateral branch) of the rubrospinal tract. This was unknown previously (Courville, 1966; Mizuno and Nakamura, 1971; Yu et al., 1972).

Monosynaptic and polysynaptic projections to orbicularis oculi motoneurons also are derived from the lateral part of the anterior and posterior interpositus nuclei, mainly ipsilaterally. Notably, interpositus neurons at these locations project to the red nucleus and to the labeled oculomotor-related nuclei (interstitial nucleus of Cajal, nucleus of Darkschewitsch, oculomotor interneurons, superior colliculus) (Fanardjian and Manvelyan, 1984; Gonzalo-Ruiz and Leichnetz, 1987). This double-projecting system probably is involved in regulating and/or reinforcing eyelid responses by exciting the rubrofacial pathway and disfacilitating the (antagonist) eyelid levator palpebrae muscle (Gruart et al., 2000b). Moreover, the interpositus nuclei project to the medullary reticular formation and other labeled brainstem structures (Mehler, 1983; Rubertone et al., 1990; Voogd, 1995). Evidence of polysynaptic connections to orbicularis oculi motoneurons from the medial and lateral cerebellar nuclei also was obtained. Labeling of cerebellar nuclei is in keeping with the involvement of motor cortex, red nucleus, and reticular formation in eyelid motor control. At later time points consistent with additional steps of transfer, labeling appeared, with a zonal distribution, in vermal and paravermal (c_1–c_3 zones) Purkinje cells. Notably, the c_1–c_3 zones have been related to trigeminally evoked eyelid blinks (Gruart et al., 1997).

Higher order forebrain structures

Cerebral cortical areas and hypothalamic and thalamic nuclei were labeled starting from 4 d, consistent with polysynaptic connections with orbicularis oculi motoneurons. Correspondingly, cortical afferents to facial motoneurons in the cat are not mono-

synaptic but reach them through the trigeminal nuclei and/or the nearby reticular formation (Fanardjian and Manvelyan, 1987a). Labeling was restricted to corticofugal pyramidal cells in layer V. Parietal cortex labeling was bilateral, with a contralateral dominance. Bilateral cortical projections to the orbicularis oculi division of the facial nucleus exist in other mammals, including humans (Morecraft et al., 2001). In a study of the early gene c-*fos* expression during classical conditioning of eyelid responses, wide areas of parietal cortex were labeled (Gruart et al., 2000c). However, labeling was restricted to nonpyramidal cells located mainly in layers 2 and 3. Apparently, layer V pyramidal cells, which as shown here represent the highest level of eyelid motor control, are not involved in this plastic response.

REFERENCES

Aou S, Woody CD, Birt D (1992) Changes in the activity of units of the cat motor cortex with rapid conditioning and extinction of a compound eye blink movement. J Neurosci 12:549–559.

Berger TW, Rinaldi P, Weisz DJ, Thompson RF (1983) Single-unit analysis of different hippocampal cell types during classical conditioning of rabbit nictitating membrane response. J Neurophysiol 50:1197–1219.

Berthier NE, Moore JW (1986) Cerebellar Purkinje cell activity related to the classically conditioned nictitating membrane response. Exp Brain Res 63:341–350.

Berthier NE, Moore JW (1990) Activity of deep cerebellar nuclear cells during classical conditioning of nictitating membrane extension in rabbits. Exp Brain Res 83:44–54.

Bour LJ, Aramideh M, De Visser BW (2000) Neurophysiological aspects of eye and eyelid movements during blinking in humans. J Neurophysiol 83:166–176.

Bracha V, Bloedel JR (1996) The multiple-pathway model of circuits subserving the classical conditioning of withdrawal reflexes. In: The acquisition of motor behavior in vertebrates (Bloedel JR, Ebner TJ, Wise SP, eds), pp 175–204. Cambridge, MA: MIT.

Courville J (1966) Rubrobulbar fibres to the facial nucleus and the lateral reticular nucleus (nucleus of the lateral funiculus). An experimental study in the cat with silver impregnation methods. Brain Res 1:317–337.

Delgado-García JM (1998) Output-to-input approach to neural plasticity in vestibular pathways. Otolaryngol Head Neck Surg 119:221–230.

Delgado-García JM, del Pozo F, Spencer RF, Baker R (1988) Behavior of neurons in the abducens nucleus of the alert cat. III. Axotomized motoneurons. Neuroscience 24:143–160.

Domingo JA, Gruart A, Delgado-García JM (1997) Quantal organization of reflex and conditioned eyelid responses. J Neurophysiol 78:2518–2530.

Erzurumlu RS, Killackey HP (1979) Efferent connections of the brainstem trigeminal complex with the facial nucleus of the rat. J Comp Neurol 188:75–86.

Evinger C, Manning KA, Sibony PA (1991) Eyelid movements. Mechanisms and normal data. Invest Ophthalmol Vis Sci 32:387–400.

Fanardjian VV, Manvelyan LR (1984) Peculiarities of cerebellar excitation of facial nucleus motoneurons. Neurosci Lett 49:265–270.

Fanardjian VV, Manvelyan LR (1987a) Mechanisms regulating the activity of facial nucleus motoneurons. III. Synaptic influences from the cerebral cortex and subcortical structures. Neuroscience 20:835–843.

Fanardjian VV, Manvelyan LR (1987b) Mechanisms regulating the activity of facial nucleus motoneurons. IV. Influences from the brainstem structures. Neuroscience 20:845–853.

Faulkner B, Brown TH, Evinger C (1997) Identification and characterization of rat orbicularis oculi motoneurons using confocal laser scanning microscopy. Exp Brain Res 116:10–19.

Fort P, Sakai K, Luppi P-H, Salvert D, Jouvet M (1989) Monoaminergic, peptidergic, and cholinergic afferents to the cat facial nucleus as evidenced by a double immunostaining method with unconjugated cholera toxin as a retrograde tracer. J Comp Neurol 283:285–302.

Gonzalo-Ruiz A, Leichnetz GR (1987) Collateralization of cerebellar efferent projections to the paraoculomotor region, superior colliculus, and medial pontine reticular formation in the rat: a fluorescent double-labeling study. Exp Brain Res 68:365–378.

Gormezano I, Kehoe EJ, Marshall BS (1983) Twenty years of classical conditioning research with rabbits. Prog Psychobiol Physiol Psychol 10:197–275.

Graf W, Gerrits N, Yatim-Dhiba N, Ugolini G (2002) Mapping the oculomotor system: the power of transneuronal labeling with rabies virus. Eur J Neurosci 15:1557–1562.

Gruart A, Blázquez P, Delgado-García JM (1995) Kinematics of spontaneous, reflex, and conditioned eyelid movements in the alert cat. J Neurophysiol 74:226–248.

Gruart A, Pastor AM, Armengol JA, Delgado-García JM (1997) Involvement of cerebellar cortex and nuclei in the genesis and control of unconditioned and conditioned eyelid motor responses. Prog Brain Res 114:511–528.

Gruart A, Schreurs BG, Domínguez del Toro E, Delgado-García JM (2000a) Kinetic and frequency-domain properties of reflex and conditioned eyelid responses in the rabbit. J Neurophysiol 83:836–852.

Gruart A, Guillazo-Blanch G, Fernández-Mas R, Jiménez-Díaz L, Delgado-García JM (2000b) Cerebellar posterior interpositus nucleus as an enhancer of classically conditioned eyelid responses in alert cats. J Neurophysiol 84:2680–2690.

Gruart A, Morcuende S, Martínez S, Delgado-García JM (2000c) Involvement of cerebral cortical structures in the classical conditioning of eyelid responses in rabbits. Neuroscience 100:719–730.

Hinrichsen CFL, Watson CD (1983) Brain stem projections to the facial nucleus of the rat. Brain Behav Evol 22:153–163.

Hiraoka M, Shimamura M (1977) Neural mechanisms of the corneal blink reflex in cats. Brain Res 125:265–275.

Holstege G, Tan J, Van Ham J, Bos A (1984) Mesencephalic projections to the facial nucleus in the cat. An autoradiographical tracing study. Brain Res 311:7–22.

Holstege G, van Ham JJ, Tan J (1986a) Afferent projections to the orbicularis oculi motoneuronal cell group. An autoradiographical tracing study in the cat. Brain Res 374:306–320.

Holstege G, Tan J, van Ham JJ, Graveland GA (1986b) Anatomical observations on the afferent projections to the retractor bulbi motoneuronal cell group and other pathways possibly related to the blink reflex in the cat. Brain Res 374:321–334.

Holstege G, Tan J, Van Ham (1988) Anatomical observations on afferent projections of orbicularis oculi and retractor bulbi motoneuronal cell groups and other pathways possibly related to the blink reflex in the cat. In: Cellular mechanisms of conditioning and behavioral plasticity (Woody CD, Alkon DL, McGaugh JL, eds), pp 273–286. New York: Plenum.

Huisman AM, Kuypers HGJM, Verburgh CA (1981) Quantitative differences in collateralization of the descending spinal pathways from red nucleus and other brain stem cell groups in rat as demonstrated with the multiple fluorescent retrograde tracer technique. Brain Res 209:271–286.

Huisman AM, Kuypers HGJM, Verburgh CA (1982) Differences in collateralization of the descending pathways from red nucleus and other brain stem cell groups in cat and monkey. Prog Brain Res 57:186–217.

Inagaki M, Takeshita K, Nakao S, Shiraishi Y, Oikawa T (1989) An electrophysiologically defined trigemino-reticulo-facial pathway related to the blink reflex in the cat. Neurosci Lett 96:64–69.

Isokawa-Akesson M, Komisaruk BR (1987) Difference in projections to the lateral and medial facial nucleus: anatomically separate pathways for rhythmical vibrissae movements in rats. Brain Res 65:385–398.

Itoh K, Takada M, Yasui Y, Mizuno N (1983) A pretectofacial projection in the cat: a possible link in the visually triggered blink reflex pathways. Brain Res 275:332–335.

Keifer J (1993) *In vitro* eye-blink reflex model: role of excitatory amino acids and labeling of network activity with sulforhodamine. Exp Brain Res 97:239–253.

Kelly RM, Strick PL (2000) Rabies as a transneuronal tracer of circuits in the central nervous system. J Neurosci Methods 103:63–71.

Kim JJ, Thompson RF (1997) Cerebellar circuits and synaptic mechanisms involved in classical eye blink conditioning. Trends Neurosci 20:177–181.

Köbbert C, Apps, Bechmann I, Lanciego JL, Mey J, Thanos S (2000) Current concepts in neuroanatomical tracing. Prog Neurobiol 62:327–351.

Kugelberg E (1952) Facial reflexes. Brain 75:385–396.

Kuypers HGJM, Huisman AM (1984) Fluorescent neuronal tracers. Adv Cell Neurobiol 5:307–340.

Kuypers HGJM, Ugolini G (1990) Viruses as transneuronal tracers. Trends Neurosci 13:71–75.

López DE, Saldaña E, Nodal FR, Merchán MA, Warr WB (1999) Projections of cochlear root neurons, sentinels of the rat auditory pathway. J Comp Neurol 415:160–174.

Magariños-Ascone C, Núñez A, Delgado-García JM (1999) Different discharge properties of rat facial nucleus motoneurons. Neuroscience 94:879–886.

Martin MR, Lodge D (1977) Morphology of the facial nucleus on the rat. Brain Res 123:1–12.

May PJ, Vidal P-P, Baker R (1990) Synaptic organization of the tectal–facial pathways in cat. II. Synaptic potentials following midbrain tegmentum stimulation. J Neurophysiol 64:381–402.

McCormick DA, Thompson RF (1984) Cerebellum: essential involvement in the classically conditioned eyelid response. Science 223:296–299.

McCormick DA, Lavond DG, Thompson RF (1982) Concomitant classical conditioning of the rabbit nictitating membrane and eyelid responses: correlations and implications. Physiol Behav 28:769–775.

Mehler WR (1983) Observations on the connectivity of the parvocellu-

lar reticular formation with respect to a vomiting center. Brain Behav Evol 23:63–80.
Mesulam MM (1982) Principles of horseradish peroxidase neurohistochemistry and their applications for tracing neural pathways—axonal transport, enzyme histochemistry and light microscopic analysis. In: Tracing neural connections with horseradish peroxidase (Mesulam MM, ed), pp 1–153. Chichester, UK: Wiley.
Mizuno N, Nakamura Y (1971) Rubral fibers to the facial nucleus in the rabbit. Brain Res 28:545–549.
Morecraft RJ, Louie JL, Herrick JL, Stilwell-Morecraft KS (2001) Cortical innervation of the facial nucleus in the nonhuman primate. A new interpretation of the effects of stroke and related subtotal brain trauma on the muscles of facial expression. Brain 124:176–208.
Múnera A, Gruart A, Muñoz MD, Fernández-Mas R, Delgado-García JM (2001) Hippocampal pyramidal cells activity encodes conditioned stimulus predictive value during classical conditioning in alert cats. J Neurophysiol 86:2571–2582.
Panneton WM, Burton H (1981) Corneal and periocular representation within the trigeminal sensory complex in the cat studied with transganglionic transport of horseradish peroxidase. J Comp Neurol 199:327–344.
Paxinos G, Watson C (1986) The rat brain in stereotaxic coordinates. New York: Academic.
Pellegrini JJ, Horn AK, Evinger C (1995) The trigeminally evoked blink reflex. I. Neuronal circuits. Exp Brain Res 107:166–180.
Rubertone JA, Haroian AJ, Vincent SL, Mehler WR (1990) The rat parvocellular reticular formation. I. Afferents from the cerebellar nuclei. Neurosci Lett 119:79–82.
Ruigrok TJH, Cella F (1995) Precerebellar nuclei and red nucleus. In: The rat nervous system (Paxinos G, ed), pp 277–308. San Diego: Academic.
Shaw MD, Baker R (1983) Direct projections from vestibular nuclei to facial nucleus in cats. J Neurophysiol 50:1265–1280.
Sinex DG, López DE, Warr WB (2001) Electrophysiological responses of cochlear root neurons. Hear Res 158:28–38.
Strominger RN, McGiffen JE, Strominger NL (1987) Morphometric and experimental studies of the red nucleus in the albino rat. Anat Rec 219:420–428.
Takada M, Itoh K, Yasui Y, Mitani A, Nomura S, Mizuno N (1984) Distribution of premotor neurons for orbicularis oculi motoneurons in the cat, with particular reference to possible pathways for blink reflex. Neurosci Lett 50:251–255.
Takeuchi Y, Nakano K, Uemura M, Matsuda K, Matsushima R, Mizuno N (1979) Mesencephalic and pontine afferent fiber system to the facial nucleus in the cat: a study using the horseradish peroxidase and silver impregnation techniques. Exp Neurol 66:330–342.
Tang Y, Rampin O, Giuliano F, Ugolini G (1999) Spinal and brain circuits to motoneurons of the bulbospongiosus muscle: retrograde transneuronal tracing with rabies virus. J Comp Neurol 414:167–192.
Thompson RF, Krupa DJ (1994) Organization of memory traces in the mammalian brain. Annu Rev Neurosci 17:519–549.
Travers JB (1995) Oromotor nuclei. In: The rat nervous system (Paxinos G, ed), pp 239–255. San Diego: Academic.
Travers JB, Norgren R (1983) Afferent projections to the oral motor nuclei in the rat. J Comp Neurol 220:280–298.
Trigo JA, Gruart A, Delgado-García JM (1999) Discharge profiles of abducens, accessory abducens, and orbicularis oculi motoneurons during reflex and conditioned blinks in alert cats. J Neurophysiol 81:1666–1684.
Ugolini G (1992) Transneuronal transfer of herpes simplex virus type 1 (HSV 1) from mixed limb nerves to the CNS. I. Sequence of transfer from sensory, motor and sympathetic nerve fibers to the spinal cord. J Comp Neurol 326:527–548.
Ugolini G (1995a) Transneuronal tracing with α-herpes viruses: a review of the methodology. In: Viral vectors: gene therapy and neuroscience applications (Keplitt M, Loewy AD, eds), pp 293–317. New York: Academic.
Ugolini G (1995b) Specificity of rabies virus as a transneuronal tracer of motor networks: transfer from hypoglossal motoneurons to connected second-order and higher order central nervous system cell groups. J Comp Neurol 356:457–480.
Ugolini G, Kuypers HGJM, Strick PL (1989) Transneuronal transfer of herpes virus from peripheral nerves to cortex and brainstem. Science 243:89–91.
Ugolini G, Morcuende S, Delgado-García JM (1999) Brainstem and cerebellar centres mediating neural control of orbicularis oculi motoneurons: retrograde transneuronal tracing with rabies virus. Soc Neurosci Abstr 25:1403.
Van Ham JJ, Yeo CH (1996) Trigeminal inputs to eye blink motoneurons in the rabbit. Exp Neurol 142:244–257.
Vidal P-P, May PJ, Baker R (1988) Synaptic organization of the tectal-facial pathways in the cat. I. Synaptic potentials following collicular stimulation. J Neurophysiol 60:769–797.
Voogd J (1995) Cerebellum. In: The rat nervous system (Paxinos G, ed), pp 309–352. San Diego: Academic.
Welsh JP (1992) Changes in the motor pattern of learned and unlearned responses following cerebellar lesions: a kinematic analysis of the nictitating membrane reflex. Neuroscience 47:1–19.
Woody CD (1986) Understanding the cellular basis of memory and learning. Annu Rev Psychol 37:433–493.
Yu H, DeFrance JF, Iwata N, Kitai ST, Tanaka T (1972) Rubral inputs to the facial motoneurons in cat. Brain Res 42:220–224.